POLITECNICO DI TORINO
Repository ISTITUZIONALE

Design and Performance Analysis of a Spherical UGV Powered by Pendulum and Control Moment Gyroscopes for Planetary Exploration

(Article begins on next page)

14 March 2025

IAC-24-A3.IP.35.x83859

Design and Performance Analysis of a Spherical UGV Powered by Pendulum and Control Moment Gyroscopes for Planetary Exploration

Francesco Di Stefano, Paolo Gualberto, Laura Salamina, Davide Sorli, Mario Troise, Matteo Melchiorre*.

Department of Mechanical and Aerospace Engineering, Politecnico di Torino, C.so Duca degli Abruzzi 24, Turin, Italy, francesco.distefano@studenti.polito.it, paolo.gualberto@studenti.polito.it , laura.salamina@polito.it , davide.sorli@polito.it , mario.troise@polito.it ,
* Corresponding Author

Abstract

Spherical robots are an emerging class of Unmanned Ground Vehicle (UGV) that is becoming attractive for space exploration for the possibility to deal with extreme planetary surface conditions. In fact, because of the shape, internal components and sensors can be protected from the outside, and the system is prevented from overturning. The work presents the advances in the design of a spherical UGV for planetary surface explorations. The robot is made of a spherical shell that encloses a locomotive system, related electronics and dedicated sensors to navigate and collect data, such as images, pressure, humidity, temperature, radioactivity and gas composition. The locomotion system that is responsible for rolling is based on a single-pendulum differential-driven mechanism, enhanced by Control Moment Gyroscopes (CMG). This solution allows for a greater torque compared to robots powered by single pendulum only, and improves capabilities against obstacles, in particular steps. In fact, for pendulum mechanisms, the driving torque depend on the barycentre offset on the radial direction, which is theoretically confined to the sphere radius. The concept described in this work add the gyroscopic torque produced by a pair of flywheels. Coupling CMG and single pendulum mechanisms has some technical challenges. The current version of the spherical robot has a diameter of 0.5 m and a mass of 22 kg, so that it can be stored into existing landers, even in multiple units. Fitting the hybrid mechanism within such a compact size, together with power and control electronics, required an iterative design, that considered the actual space available inside the shell and the desired performance of the robot. The paper summarizes design methods, parts dimensioning, mechatronic integration, control and energy balance of the pendulum-CMG system. The design is supported by numerical models of the subsystems, like gyroscopes, pendulum and transmission. Multibody simulations of the complete system analyse the motion of the robot rolling on straight trajectories, curved paths and steps. Performance analysis of the proposed locomotion system shows significant improvements compared to classical single pendulum version. The result is a spherical robot that can run up to 2.5 m/s, climb slope of 15° and overcome steps that are 10 times higher with respect to single pendulum robots of the same size. An energetic analysis is carried out to evaluate autonomy in relevant mission profiles.

Keywords: spherical robot, UGV, space exploration, robot design, robot modeling

1. Introduction

This paper presents the advances of the Spherical Rover (SR) for planetary exploration introduced in [1], and developed by [2]. The rover is designed to satisfy a number of requirements that are in line with exploration missions. In particular, it is equipped with dedicated sensors, and it can run different types of terrain. The driving mechanism is based pendulum and Control Moment Gyroscopes (CMG) and allows to overcome obstacles such as steps and inclines [1]. Compared to traditional counterparts such as wheeled and legged Unmanned Ground Vehicles (UGV), this rover has several advantages that are specific of SRs, such as: prevention from tipping, better resistance to shocks, enclosed mechanism and sensors, less friction with the ground, and downhill energy savings.

With respect to the state of the art of SRs, a comprehensive overview of existing types of SRs was made in the recent publication [2]. A classification can be made on the basis of the rolling principle. The main families that can be identified are: Barycenter offset (BCO), where actuation takes place by displacing the Center of Mass (COM) of the system; Shape Transforming (ST), where motion is achieved by external shell reconfiguration; Angular Momentum (AM), that exploits reaction wheels or CMG for rolling.

The most popular system is the BCO because of its simplicity. One mechanism that exploits BCO is the Hamster Ball (HB), whose driving system consists of a single/multi wheeled mobile robot placed inside the spherical shell that climbs up the internal surface of the sphere [3]. The major drawback of HB is that collision

with obstacles may cause the loss of contact between wheels and internal surface and this may lead to internal structure overturning. This also implies that shell cannot be flexible. Moreover, omnidirectionality is not always guaranteed since depends on the implemented system [4], [5]. Another example of BCO system is the Unbalanced Masses (UM), that consists of a number of masses that translate in a controlled manner along linear guides inside the sphere [6], [7]. Compared with HBs, UMs better withstand shocks, since they do not have a wheel in contact with the shell, but they still suffer from the impossibility of having a flexible shell, as the frame which support the masses must be rigid. In addition, controlled rolling requires that masses undergo continuous acceleration, so robots using UMs require powerful actuators and are therefore inefficient. One system that solves the above problems is the Pendulum-Driven (PD), which consists of a mass hanging from a diametric shaft [8], [9], [10]. The pendulum, however, in its basic version, is not omnidirectional, i.e. the robot, starting from a standstill, cannot take any direction. There are, however, double pendulum versions in which quasi or full omnidirectionality is achieved [11], but at the cost of high design and control complexity.

Considering pros and cons of the various systems just mentioned, combined with performance requirements, the trade-off in [1] led to the design of a spherical robot equipped with a 2 Degrees Of Freedom (DOFs) pendulum. In particular, the version [1] had a 0.5 m diameter and a maximum mass of 25 kg. These features were defined to provide space for an array of sensors, while at the same time maintaining dimensions that allow the robot to be easily carried by hand, for terrestrial applications, or by a lander, for space applications. The maximum velocity of 2.5 m/s was defined to be comparable to human average stroke. A remote-control feature was considered for tele-operated implementations.

Version [1], while introducing interesting innovations, including a differential-based transmission that revisits the idea by Schroll [12] but with a more compact construction solution, had a major drawback: the intrinsic limit of BCOs. Indeed, the maximum torque of BCOs depends on the offset of the COM relative to the centre of the sphere. Since the system is contained within the spherical shell, there is an intrinsic limit to this offset. Theoretically, this offset is represented by the radius R, but in practice, it ranges from 0.4 to 0.5 R. In [1], for example, an offset of 0.45 R was achieved, resulting in a maximum step height of 25 mm.

To overcome this significant limitation, version [2] aimed to expand the existing design with a CMG system (see Fig. 1). The improved version is thus hybrid, utilizing a pendulum system for rolling and,

when necessary, activating the CMGs to provide a temporary torque boost. This has allowed it to overcome steps up to 4 times higher, up to 100 mm. In [2], the steps leading to the conceptualization of the hybrid robot are described, and a control scheme for straight trajectories is also proposed. However, despite presenting an advanced concept compared to the first version [1], work [2] is not exhaustive, as it misses the electronic design and curved path control.

This article presents the revision of the mechanical design of version [2], the design of the electronics, the multibody model of the full robot, and an improvement in the control system which now also considers curved trajectories.
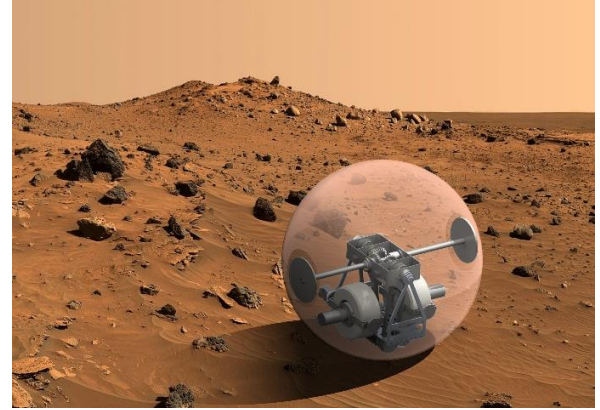

Fig. 1. An illustrative image of the pendulum-CMG spherical robot [2], which reveals the internal mechanism.

2. Recall to the driving principle

It is well known that the obstacle crossing capability for BCO spherical robots is related to geometry and inertial properties. In general, obstacles can be intended as inclines or steps. However, in [1] it is shown that the worst condition, which then becomes the design relation, is that of the spherical robot in the presence of a step. For example, consider a pendulum-actuated SR. Let a denote the offset of the barycentre of the system G relative to the centre of the sphere S, as sketched in Fig. *2*. It is straightforward to write down the equation that relates the maximum step h to geometrical and inertial properties of the robot:

$$\frac{h}{R} = 1 - \sqrt{1 - \left(\frac{a}{R}\right)^2} \qquad (1)$$

From (1), if the radius is fixed because of a maximum size requirement, the only parameter to be optimized is the offset a. In [1], a differential mechanism was used to mount the actuators on the pendulum, close to the shell, so to increase a; in fact, the greater the offset, the higher the step h. However, it was observed that it is not possible to achieve high step climbing by pendulum implementation only.
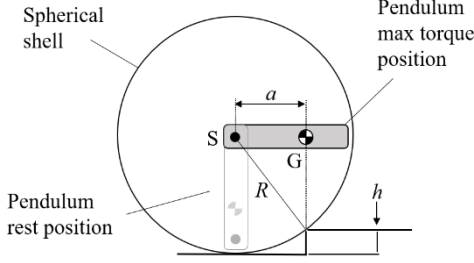
Fig. 2. Step climbing situation in limit condition. To overcome the obstacle, system's barycentre must be placed over the step edge.

In order to enhance step climbing performance, a pair of CMGs were introduced in [2]. In particular, the torque τ_G that can be provided by a scissored-pair CMGs can be written as:

$$\vec{\tau_G} = 2 \cdot I_{fl} \, \vec{\omega} \wedge \vec{\Omega_t} \qquad (2)$$

where I_{fl} is the flywheel moment of inertia, ω is the spinning speed of each flywheel along its symmetry axis and Ω_t is the tilting speed simultaneously applied along a perpendicular axis.

From [1], by rising the pendulum to the maximum torque position and by activating the CMGs, the maximum step can be written as:

$$\frac{h}{R} = 1 - \sqrt{1 - \left(\frac{a + \frac{\tau_G}{(m_p + M_s)g}}{R}\right)^2} \qquad (3)$$

Equation (3) quantifies the increasing of the ratio h/R due to the gyroscopic torque, with respect to the case of pendulum only, expressed by (1).

The combination between pendulum and CMG propulsion takes the main advantages from both these systems. The main structure is still a pendulum for optimal and responsive control of the rover. However, by actuating CMGs it is possible to noticeably increase the torque acting on the shell, allowing higher step to be climbed.

3. Design
3.1 Mechanical design
The mechanical design was fully defined to withstand the stresses arising from the main working points and considering the positioning of the electronics within the rover. The parts to be fabricated were properly dimensioned, and off the shelf (OTS) components were identified. Moreover, the design took into account also the assemblage feasibility.

3.1.1 Revision of the pendulum subsystem
The rotation between pendulum and spherical shell is decoupled by a 2 DOFs gimbal, which is shown in Fig. 3. The gimbal chassis hosts transmission components, that are made of a differential gear,

actuated by two pulleys. The design of this subsystem has been maintained as it is compact and made of OTS components, except the chassis, which must be fabricated apart.

The input torque is transmitted to the pulleys by two DC motors, placed at the bottom of the pendulum structure, through timing belts. Unlike the gimbal, the pendulum structure required a revision in order to withstand the forces in worst case conditions, and to host electronics. For instance, the previous version of the pendulum structure, from [2], is shown in

Fig. 4.: it was made of a lightweight structure, designed on a purely functional level. Main motors and CMGs were placed at the bottom to lower the system's COM, allowing higher torques to be achieved. Another key aspect to notice is the symmetry of the design. An unbalanced distribution of masses would lead to an angular offset in the pendulum's rest position, making the controller more complex to design. Finally, the central space was left empty to allow the CMGs rotation when implementing the gyroscopic maneuver.
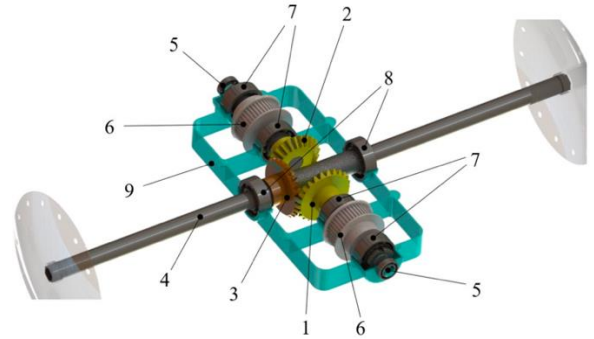

Fig. 3 Design solution of the differential gear. 1)-2) Sun gears; 3) Planet gear; 4) Main rover shaft; 5) Steer shaft; 6) Pulley; 7) Steer shaft bearing; 8) Drive shaft bearing; 9) Chassis.
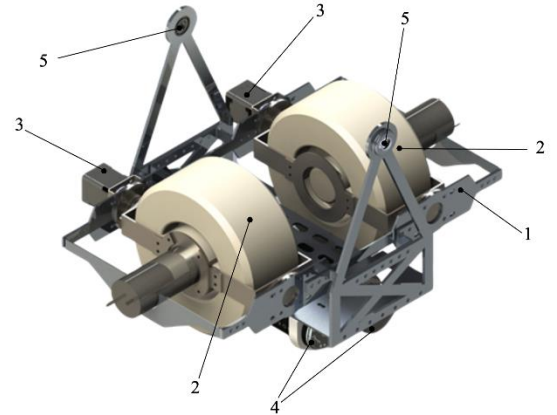

Fig. 4. Inherited pendulum design from [2]. 1) Pendulum structure; 2) CMG groups; 3) Stepper

motors; 4) Pendulum main motors; 5) Connection to steer shaft bearings.

A further study was carried out under conservative assumptions, and taking into account the maximum torque configuration of pendulum and CMG. All structural parts were studied by means of Finite Element Analysis (FEA), defining geometry and material. The final design of the pendulum is shown in Fig. 5. The structure is made of aluminum, except for the side plates, which is made of steel. The latter has been redesigned to withstand the stresses in the connections to steer shaft. In addition to an improvement of the existing components, batteries and their cases, 3D printed in PLA, are also shown in the assembly, fixed to the lower part of side plates.
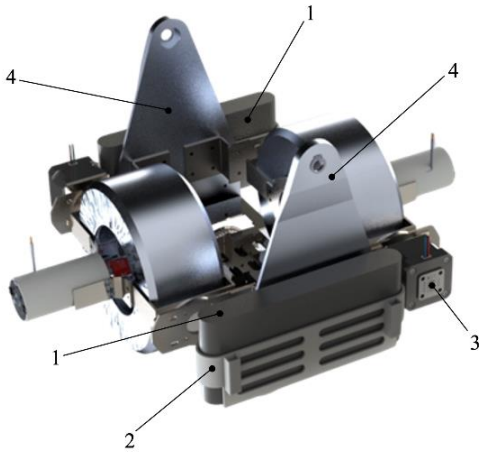

Fig. 5. Pendulum final design. 1) Battery packs; 2) Battery case; 3) Stepper magnetic encoder; 4) Pendulum side plates.

3.1.2 Revision of the CMG subsystem

The gyroscopic subsystem comprises the flywheel and its associated motors. The system's design is illustrated in Fig. 6. In the assembly, part one half of the flywheel cover has been sectioned to show the inside. Since inertia depends on both geometry and density of the body, stainless steel was selected to satisfy the required flywheel inertia once the sizing process was completed. The same material was selected also for structural parts, such as titling plates, connections to pendulum structure and shaft. The coupling between the spinning motor and the shaft is realized through an elastic joint. The gyro case is realized in aluminum alloy, it provides structural support and user safety, minimizing drag friction. It is split into two halves for easy assembly, connected by screws and plates. The connection with the pendulum structure is performed symmetrically using bearings, reducing the load on the stepper motor shaft.
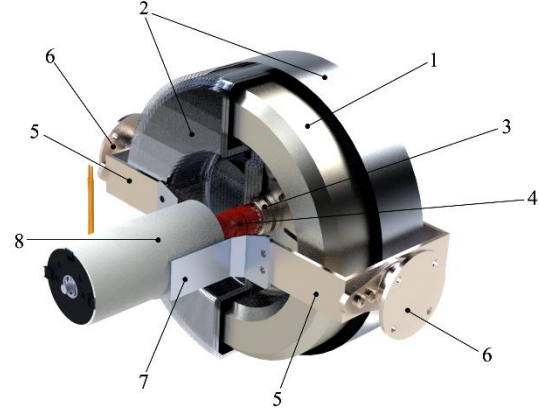

Fig. 6. CMG group final design. 1) Flywheel; 2) Carters; 3) Bearings to decouple flywheel and carter motion; 4) Jaw coupling; 5) Tilting plates; 6) Bearing connection to pendulum structure; 7) Spinning motor housing; 8) Stepper motor.

3.1.3 Revision of the spherical shell

The pendulum hangs on the diametral main shaft of the sphere. The joint system between the main shaft and the shell was developed to simplify the assembly of the rover. Each joint requires 12 screws for attachment with the shell and one screw for attachment with the main shaft end. Once the pendulum has been assembled together with the differential gearbox and the main shaft, the structure can be placed on the lower half of the spherical shell, by positioning the main shaft on the side joints, and secured with screws at the ends of the shaft (see Fig. 7). Finally, the upper half of the shell can be attached to the rest of the assembly.

There are holes in the centre of the junction parts to connect cables from the battery to a charging unit. In fact, a need that arose during the construction of the rover was to be able to recharge the batteries without disassembling the shell. The challenge is that the pendulum and the main shaft are in a state of relative rotation when the robot moves forward. Since the batteries are placed in the lower part of the pendulum, cable would twist around the main shaft and eventually break. To address this point, Bore slip rings are mounted on each side of the main shaft of the rover, in the proximity of the connection with the shell.

3.1.4 OTS components

Off-the-Shelf (OTS) components (Table 1) were selected on the basis on working conditions, and in order to minimize sizes. The acrylic shell was chosen to show the internal mechanism. A rubber membrane or a shell of a different material and finish is required to have sufficient friction with the ground for advancement.
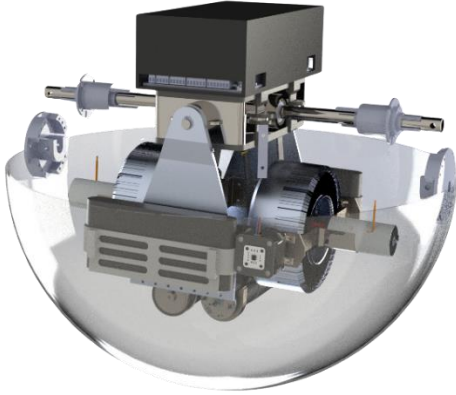
Fig. 7. Mounting the pendulum assembly on the lower half of the shell.

Table 1. OTS mechanical components.

Components	Units
61800-2RS-SKF bearings	4
W618-8-SKF bearings	2
61701-2RS bearings	4
6202-2RS-SKF bearings	6
ALS-014-R joint	2
POGGI 3MGT3 belts	2
GPT44GT3150-A-N12 pulleys	2
GPT44GT3150-A-N15 pulleys	2
BSM2030 miter gear	3
Acrylic cupola	2

3.2 Electronic design

In this section, power and control electronic design is presented. The whole electronic structure has been completely defined in this work, to properly power the system and to actuate the control strategy. It is possible to distinguish between four main groups: actuators, controls, sensors and power supply.

The actuators of the system are the motors selected for the pendulum tilting and for the implementation of the gyroscopic maneuver. The required motors can be divided into three main groups: a pair of pendulum main motors, a pair of spinning motors, and a pair of tilting motors.

The choice of the pendulum motors considered the maximum continuous torque of 0.122 Nm, calculated on the base of a worst case scenario where the robot climbs a 15° incline, a peak torque of 0.391 Nm, which is derived from the maximum torque that can be exerted by pendulum plus gyroscope (only to be used for short periods), and the maximum continuous

velocity of 2.5 m/s by requirements. The required torques takes into account an efficiency of 0.67 of the transmission, derived from the previous works [2]. The selected pendulum main motors are the Maxon RE 40 with 24V as nominal voltage. Both the motors are paired with Planetary Gearhead GP 42 C, characterized by a reduction ratio of 81:1.

CMG and spinning motors are selected considering the inertia of the flywheels and their working conditions. The flywheel has a radius of 66 mm a 3.35 kg mass, and $I_{fl} = 9.8 \cdot 10^{-3}$ kg·m^2, defined so to overcome a step of 100 mm [2]. By design, the CMG groups can be tilted only for 90° to exploit the gyroscopic torque. By imposing as execution time 1s, the tilting velocity results to be Ω_t=15 rpm. Lower execution times may create noticeable vibrations, while longer execution times would consume a higher amount of energy. The spinning velocity can be computed starting from (*2*). Since the other quantities are known, it is possible to calculate a spinning speed of 7900rpm.

From these considerations, the stepper motor Nema17 with 40Ncm holding torque has been selected for tilting. Due to the lack of space, this motor cannot mount a brake, implying that it must constantly be powered to exert the required torque. The chosen spinning motor is the Maxon DCX 35 L with 12 V as nominal voltage.

In order to correctly impose a control strategy, sensors are needed to acquire feedback signals. Two IMU sensors are implemented: the first one measures the position of the sphere and both the speed and the angle of the pendulum in forward position, the second one measures both the speed and the angle in lateral position.

Position and velocity signals are provided by encodes. Two types of encoders have been mounted: the first ones are paired with pendulum main motors for speed acquisition, the second ones are paired with tilting motors for both speed and position acquisition. Finally, a transceiver sensor was selected for tele-operated control.

To properly control the motors, they are distinctly paired to the specific driver that suits for their characteristics; BTS7960 control spinning motor type, TMC2208 control the tilting motor and Maxon ESCON 50/5 is used for Maxon RE40 motors. The entire system is controlled by an Arduino Mega as microprocessor unit. This type of microprocessor has sufficient computational power to handle both straight and lateral path controllers (see Chapter 5), which implement Fuzzy PID structure.

In the Table 2 all the OTS components are listed. Although the batteries appear in this table, their selection is presented in Chapter 4. Fig. 8 shows electronics subsystems and their connections.

Table 2. Electronic OTS components

| Components	Description	Units
Maxon RE 40 +	Pendulum motor	2
Planetary Gearhead 42C	Gear reduction	
Maxon DCX 35L	Spinning motor	2
Nema17 (40Ncm)	Tilting motor	2
HEDL 5540	Pendulum encoder	2
Maxon ESCON 50/5	Pendulum Driver	2
BTS7960	Spinning motor driver	2
TMC 2208	Tilting motor driver	2
AS5600	Tiliting motor encoder	2
IMU MPU-6050	IMU sensor	2
NRF24L01	Receiver/trasmitter	1
Bore slip ring H1532	Slip Ring	2
Arduino Mega	Micro-controller	1
MaxAmps Li-Ion 5000 8S1P 28.8V	Battery	2
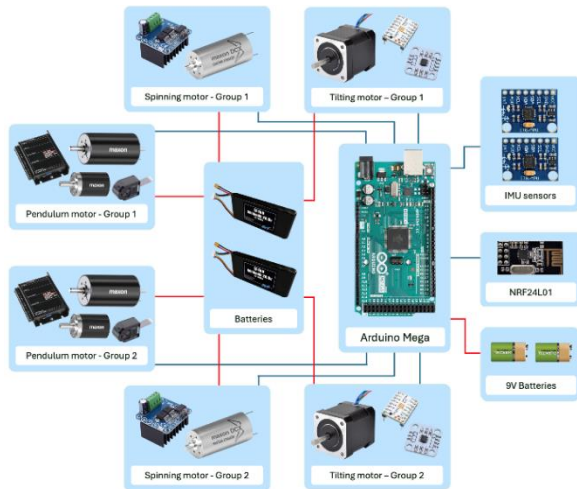
Fig. 8. Schematic of the electronics
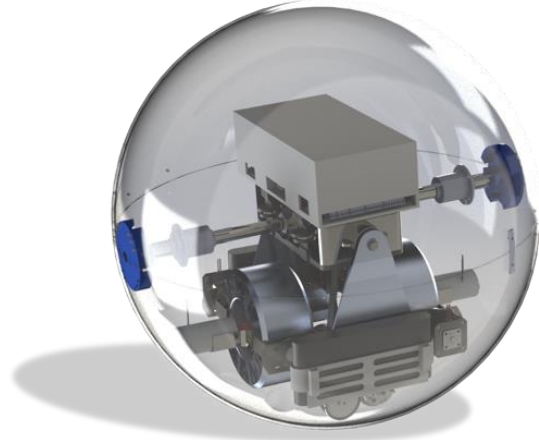
Fig. 9. Spherical rover final design.

3.3 Summary

The final design of the rover is shown in Fig. 9. At the center of the sphere, on top of the differential box, is the electronics enclosure. This component is 3D printed in ABS and contains most of the control electronics. The systems characteristics are shown in Table 3. The total mass of the rover does not exceed the initial goal and COM offset was increased respect to previous version. The final result is a rover ready for prototyping. By knowing the final design, an appropriate control strategy can be developed.

Table 3. Rover final characteristics.

Diameter	0.5 m
COM offset	0.09 m
Total mass	22.4 kg
Pendulum mass	15.65 kg

4 Energetic analysis

The study of power consumption must take into account the different cases that the rover may encounter along its path: plane, slope and step. As previously mentioned, obstacles have been modelled as slopes and steps. Thus, the study can be divided into three main situations: moving on a plane, climbing a slope of 15º, climbing a step of 100 mm. For each of these cases, the consumption of each motor was computed. The other electronic components are not included in the following analysis since they can be easily supplied by a pair of 9 V Li-Ion batteries. This guarantees sensor independence from the rest of the system.

The battery consumption is proportional to the torque required by the motors, which is determined by the working load. For planes and slopes, the consumption totally depends on the main motors to maintain the pendulum steady at a precise angle. The

required current can be computed for both these situations. In motion on a plane at constant speed, a 15° angle of the pendulum has been selected to compensate frictional forces. In the slope climbing, a 45° angle has been computed to compensate both frictional and gravity forces. In the third situation the capacity for a single step climbing has been computed. Main motors must maintain the pendulum at 90° while the spinning and tilting motors execute the gyroscopic manoeuvre.

Power consumption in each case is reported in Table 4. The battery must satisfy the maximum required voltage of 24.89 V, imposed by main motors. The best compromise between size and capacity was found in a pair of MaxAmps Li-Ion having 5000 mAh and 28.8 V. Assuming a 15° slope at a constant speed of 2.5 m/s, a duration of 50 minutes is obtained. Since this result refers to extreme working conditions, higher duration can be expected. The reported results are related to Earth gravity, thus an increase in duration is to be expected when referring to lunar or Martian gravity.

Table 4. Rover power consumption in different cases.

Scenario	Required current	Capacity
Plane	1.89 A	-
Slope	4.94 A	-
Step	-	35.23 mAh

5 Control

The control system is designed to handle different movement scenarios, including straight-line trajectories, curved paths, and obstacle climbing.

5.1 Speed controller for straight trajectory

$$\omega_3 = \frac{\omega_1 - \omega_2}{2} - \omega_p \quad (4)$$

$$\Omega = \frac{\omega_1 + \omega_2}{2} - \Omega_p \quad (5)$$

In order to realize this speed controller, the spherical robot design and kinematics equation of motion has been considered (4). They can be derived by the differential mechanism presented in [2]. The meaning of kinematics quantities are shown in Fig. 10.

Pendulum motor velocities are denoted with ω_1 and ω_2, while ω_3 and ω_p correspond to the forward sphere and pendulum angular velocity. To perform a straight-line trajectory, ω_1 and ω_2 must have same module but opposite direction. Otherwise, a lateral velocity is generated on both sphere (Ω) and pendulum (Ω_p), as shown in (5). This allows to perform curvilinear paths.
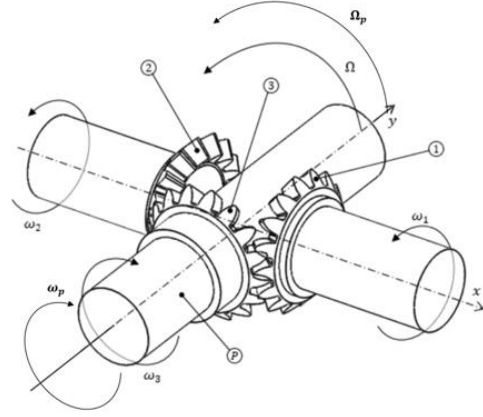

Fig. 10. Differential mechanism of the spherical rover.

A straight trajectory control strategy has been already developed in [2]. It consists of a Fuzzy PID controller supported by a PI controller activated when the velocity gets close to the reference in order to limit the overshoot response. The above control system has been re-adapted for the presented spherical robot, tuning the Fuzzy gain scheduler values with new suitable parameters. Instead, the control for curved trajectories is presented in the following section.

5.2 Lateral side angle control

A second separated controller aims at stabilizing the pendulum side angle (θ) over an angular set reference (see Fig. 11). It also controls the lateral angular velocity Ω of the rover, avoiding oscillations by imposing a 0 rad/s reference. First, the angular measurement feedback (θ_{FB}) is subtracted to the reference angle (θ_{SET}) to define the error function. A second error function is necessary to track the sphere lateral oscillation using sensor measurement feedback, then a PID controller is implemented, as shown in the Lateral path control block in Fig. 12.

The kinematics equation of motion (5) is crucial in the controller design, it is used in combination with a second PID controller opportunely tuned. The resulting output from the second PID represents the input that it is finally fed to the pendulum motors.
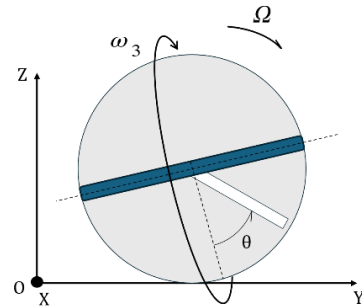

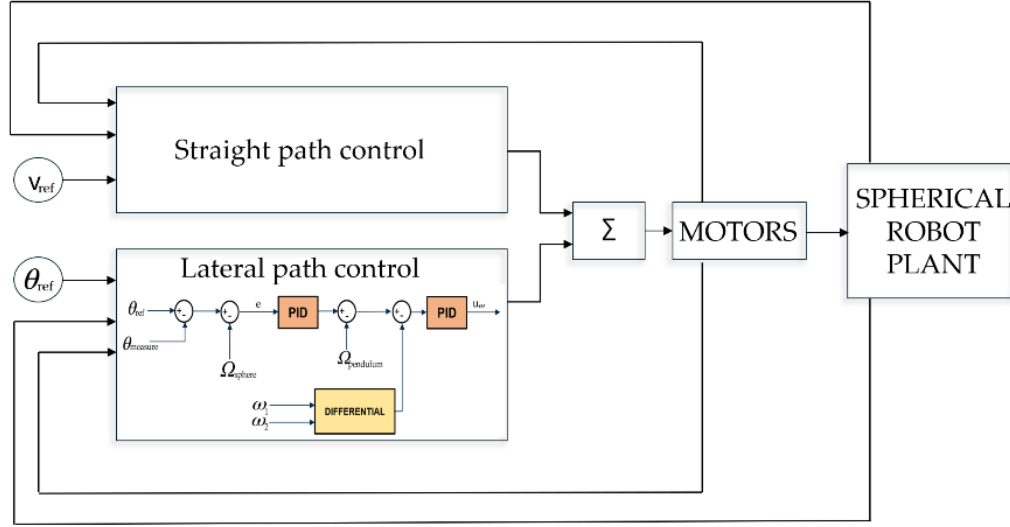Fig. 11. Functional representation of spherical robot – front view.

Fig. 12. Control scheme

5.3 Trajectory control

The final control loop suggested for motion control is a combination of the two separated controllers designed before, as shown in **Errore. L'origine riferimento non è stata trovata.**. In fact, just before the motors' block, the inputs coming from both the controllers are summed through a junction. The advantage of this controller architecture is the great performances when a curved trajectory is needed thanks to the fast response of the lateral side controller avoiding lateral oscillations. The resulting tests show the behaviour of the spherical rover in different situations.

6. Results

6.1 Simulation environment

Starting from the 3D CAD, the spherical robot is imported in Matlab Simscape Multibody to simulate the system dynamics. On the other hand, the control scheme is built in Simulink, and control and feedback signals are injected from Simulink to Simscape blocks, and vice versa.

Main pendulum DC motors have been modelled with classical resistor-inductor circuit [2], while the CMG spinning and tilting torques are directly injected in the model with source blocks. The data acquisition system comes from Simulink's "transform sensor" modules, to represent the sensors designed in Chapter 2. The data from the virtual sensors are taken as ideal and free from disturbances. Surface block is connected to the virtual rover through the Spatial contact force Simulink block and shaped occasionally as test conditions, like infinite plane, inclined one and custom surface to better represent moon or mars landscape.

Starting from the rover multibody model developed above, two different tests are presented, in order to validate the model and to compare the results with the mission requirements. Tests are conducted in the Simulink environment with DAE solver, the most suitable for Simscape models. As mentioned, the purpose of each test is following the reference linear velocity and lateral pendulum angle, considering that 'θ' is constrained by structural limitations and thus bounded between -22.15 degrees and +22.15 degrees, while the linear velocity lies in the range between -2.5 m/s and +2.5 m/s.

6.2 Straight path

Simulation and experiments are presented, specifically regarding the control performances during linear velocity tracking. In this case imposing only a linear velocity, it corresponds to provide the same angular velocity at the motors in opposite direction, that lead to raise the pendulum forward or backward and so robot runs straight trajectories.

Fig. 13 shows the simulation where the robot reference angular velocity (red line) is set to -4 rad/s after 1 second of simulation. The blue line is the real spherical robot velocity at the center of the shell, it follows the desired reference and reaches the steady state. As the potion is a pure rolling, this correspond to -1 m/s. After several experiments, all possible velocity references are tested, and the steady state behavior is guaranteed. Table 5 shows the control performances in the two most important cases. Performances are evaluated in terms of rising time, settling time 2% and overshoot.
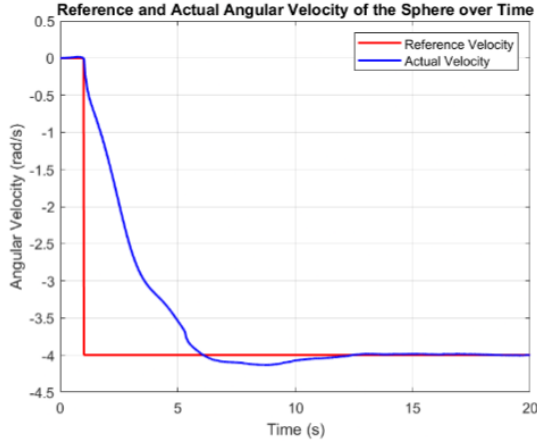
Fig. 13. Straight path control velocity tracking using a step reference input.

Table 5. Transient performances of straight path controller

Test	Rise Time (s)	Settling Time 2% (s)	Overshoot (%)
STEP input 1 m/s	5.09	9.00	3.25
STEP input 2.5 m/s	6.84	10.02	4.35

6.3 Curved path

The spherical rover, when implementing the designed planar trajectory control, can navigate over curved trajectories, just imposing the two reference values, that are robot linear velocity and pendulum lateral angle.

Fig. 15 shows in blue line a circle trajectory made by the ROVER during simulation. A 9 meters radius circle is traced with maximum error of 0.4m.

The robot from standstill position after 1 simulation second tracks -4 rad/s velocity and after 5 simulation seconds starts to reach the reference lateral pendulum angle of -10°, as can be seen in Fig. 15. Steady state performance is achieved in less than 18 s and the planar trajectory controller is validated (Fig. 16).

7. Conclusion and future works

An innovative spherical robot is presented in this research. The particular architecture constituted by a differential drive system connected to a pendulum and Control Moment Gyroscope device allow high performance given the inherent limitations of spherical robots.

A complete study of the Mechanical components and electronics system to be integrated lead the project to the state of manufacture. The energetic analysis demonstrates an entire hour of autonomy in constant operative condition with earth physical parameters setting, suggesting higher performances on planetary surfaces. After that, a high-fidelity multibody model has been developed, used for control purposes.
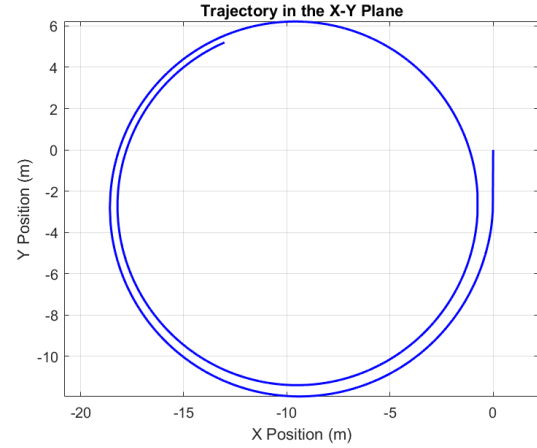

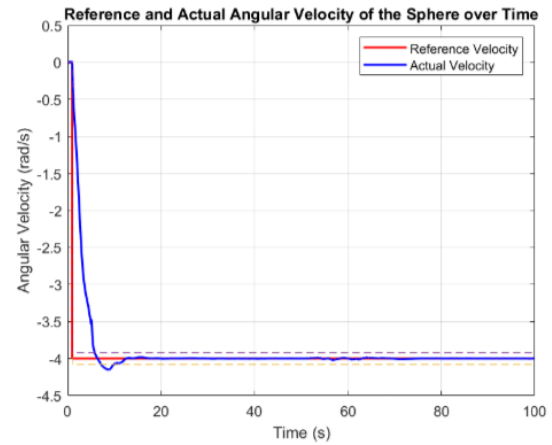Fig. 14. Circular trajectory of the rover.
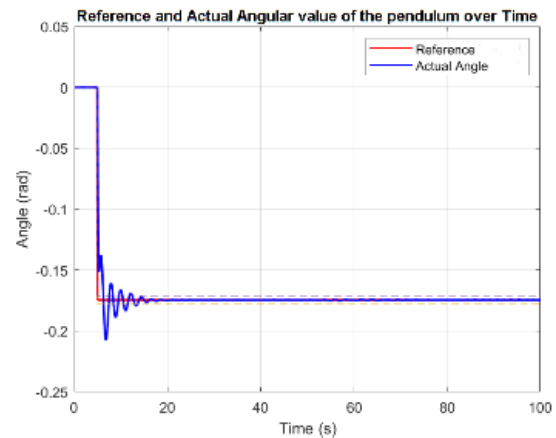

Fig. 15. Curved path velocity tracking.

Fig. 16. Curved path angle tracking.

Two control systems have been developed and merged into a single one, to track both reference linear velocity, both pendulum angle and so radius of curvature. Simulation and tests have been presented showing the robot linear and planar motion with relative performances. Future works will regard the construction of the prototype and experimental

validation, in order to develop a more robust control system, which takes into account non-idealities, such as sensor noises and disturbances. Moreover, it will be important to generate the firmware code of it to implement the code on a real micro-controller.

Bibliography

[1]   M. Melchiorre, L. Salamina, S. Mauro, and S. Pastorelli, "Design of a Spherical UGV for Space Exploration."

[2]   M. Melchiorre, T. Colamartino, M. Ferrauto, M. Troise, L. Salamina, and S. Mauro, "Design of a Spherical Rover Driven by Pendulum and Control Moment Gyroscope for Planetary Exploration," *Robotics*, vol. 13, no. 6, Jun. 2024, doi: 10.3390/robotics13060087.

[3]   M. Bujňák *et al.*, "Spherical Robots for Special Purposes: A Review on Current Possibilities," 2022. doi: 10.3390/s22041413.

[4]   J. Alves and J. Dias, "Design and control of a spherical mobile robot," 2003.

[5]   Q. Zhan, Y. Cai, and C. Yan, "Design, analysis and experiments of an omni-directional spherical robot," in *Proceedings - IEEE International Conference on Robotics and Automation*, 2011. doi: 10.1109/ICRA.2011.5980491.

[6]   S. Sang, J. Zhao, H. Wu, S. Chen, and Q. An, "Modeling and simulation of a spherical mobile robot," *Computer Science and Information Systems*, vol. 7, no. 1, 2010, doi: 10.2298/CSIS1001051S.

[7]   F. Tomik, S. Nudehi, L. L. Flynn, and R. Mukherjee, "Design, fabrication and control of spherobot: A spherical mobile robot," *Journal of Intelligent and Robotic Systems: Theory and Applications*, vol. 67, no. 2, 2012, doi: 10.1007/s10846-012-9652-2.

[8]   B. Zhao, P. Wang, H. Hu, M. Li, and L. Sun, "Study on turning in place of a spherical robot based on stick-slip principle," in *2009 IEEE International Conference on Robotics and Biomimetics, ROBIO 2009*, 2009. doi: 10.1109/ROBIO.2009.5420575.

[9]   V. Kaznov and M. Seeman, "Outdoor navigation with a spherical amphibious robot," in *IEEE/RSJ 2010 International Conference on Intelligent Robots and Systems, IROS 2010 - Conference Proceedings*, 2010. doi: 10.1109/IROS.2010.5651713.

[10]   K. Schilling *et al.*, "Band 21 Würzburger Forschungsberichte in Robotik und Telematik DAEDALUS Descent And Exploration in Deep Autonomy of Lava Underground Structures Uni Wuerzburg Research Notes in Robotics and Telematics."

[11]   M. Yang *et al.*, "Design and Analysis of a Spherical Robot with Two Degrees of Freedom Swing," in *Proceedings of the 32nd Chinese Control and Decision Conference, CCDC 2020*, 2020. doi: 10.1109/CCDC49329.2020.9164196.

[12]   by C. Gregory Schroll, C. by, and O. H. Alexander Slocum, "Design of a Spherical Vehicle with Flywheel Momentum Storage for High Torque Capabilities," 2008.